Title

Chloroquine disrupts zinc storage granules in primary Malpighian tubule cells of
Drosophila melanogaster

Authors & Affiliations

Jessica P. Campos-Blázquez,[1*] Nils Schuth,[2*] Erika Garay,[1] Adam H. Clark,[3] Urs
Vogelsang,[3] Maarten Nachtegaal,[3] Rubén G. Contreras,[1] Liliana Quintanar,[2] Fanis
Missirlis[1]

[1] Department of Physiology, Biophysics and Neuroscience, Cinvestav, 07360 Mexico
City, Mexico.
[2] Department of Chemistry, Cinvestav, 07360 Mexico City, Mexico.
[3] Paul Scherrer Institut, CH-5232 Villigen, Switzerland.

[*] These authors contributed equally to this work

Correspondence

Dr Fanis Missirlis
Avenida Instituto Politécnico Nacional 2508
Department of Physiology, Biophysics & Neuroscience
Cinvestav Zacatenco
Mexico City 03760
Mexico

fanis@fisio.cinvestav.mx

Running head

Chloroquine is not a zinc ionophore

Abstract

Contrasting reports exist in the literature regarding the effect of chloroquine treatment on cellular zinc uptake or secretion. Here we tested the effect of chloroquine administration in the *Drosophila* model organism. We show that larvae grown on a diet supplemented with 2.5 mg / mL chloroquine lose up to 50% of their stored zinc and around 10% of their total potassium content. This defect in chloroquine-treated animals correlates with the appearance of abnormal autophagolysosomes in the principal cells of the Malpighian tubules, where zinc storage granules reside. We further show that the reported increase of Fluozin-3 fluorescence following treatment of cells with 300 μM chloroquine for one hour may not reflect increased zinc accumulation, since a similar treatment in Madin-Darby canine kidney cells results in a 36% decrease in their total zinc content. Thus, chloroquine should not be considered a zinc ionophore. Zinc supplementation plus chloroquine treatment restored zinc content both *in vivo* and *in vitro*, without correcting autophagic or other ionic alterations, notably in potassium, associated with the chloroquine treatment. We suggest that chloroquine or hydroxychloroquine administration to patients could reduce intracellular zinc storage pools and be part of the drug's mechanism in of action.

Graphical Abstract
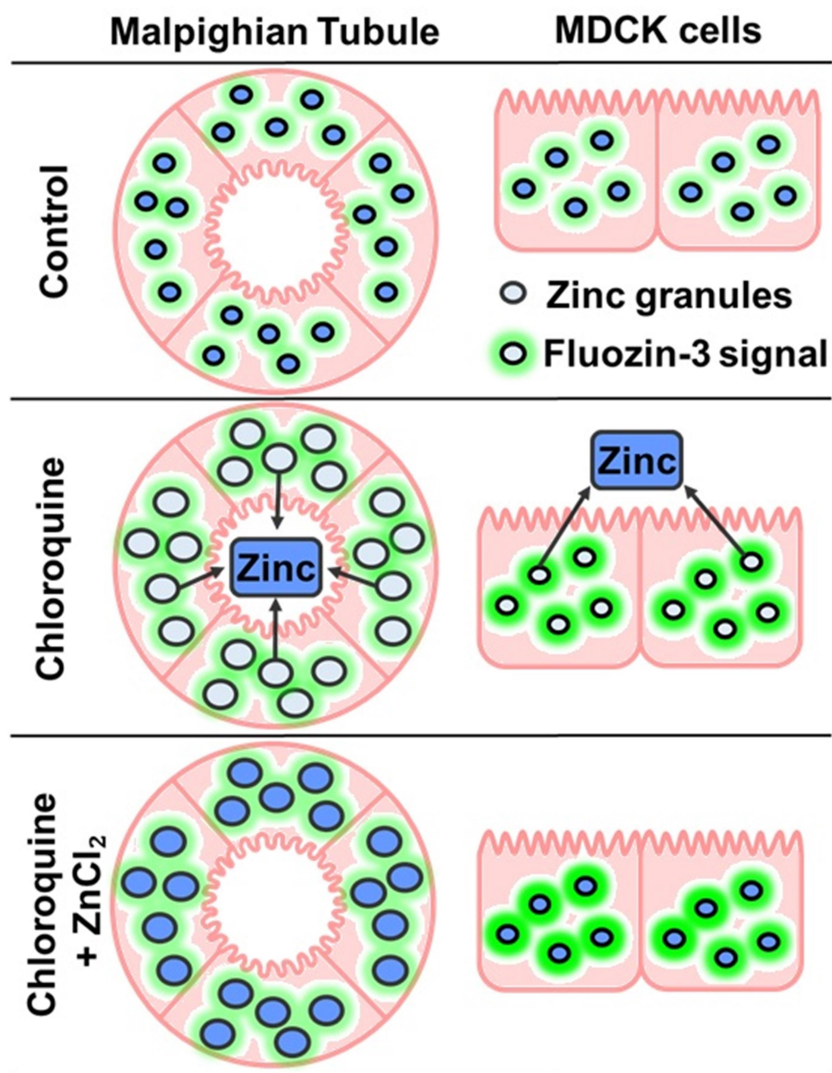
Introduction

Chloroquine was the first effective antimalarial drug [1]. Soon after, this substance was used to treat autoimmune disorders [2, 3]. Chronic use of chloroquine induces myopathy and macular degeneration [4, 5]. Hydroxychloroquine, a less toxic derivative of chloroquine, was broadly used at the onset of the Covid19 pandemic to treat SARS-Cov-2-infected individuals with disappointing results [6]. Nevertheless, hydroxychloroquine is regularly prescribed and recommended to this time for all patients with lupus erythematosus [7]. It also has many other specialized clinical uses [8].

The mechanism of action of this drug has been an area of many investigations. Chloroquine inhibits melanosome formation in tadpoles [9], affects lysosomes and autophagic processes and induces myeloid bodies (abnormal intracellular multimembrane inclusions) in rat livers [10], and inactivates lysosomal function in cultured fibroblasts [11]. Malaria-infected primates exhibited similar alterations upon chloroquine administration, primarily affecting *Plasmodium* trophozoites that concentrate hemozoin in a digestive vacuole [12]. A proposal to explain the observed effects of chloroquine on lysosomes and related structures, and also the mechanism of its cellular uptake and accumulation, was the idea that upon protonation in an acid environment, the molecule becomes membrane-impermeable, a property known as lyososomotropism [13, 14]. It was further postulated that an increase in lysosomal pH, also reported in cells treated with chloroquine [15], could be the direct effect of the above-mentioned protonation by simple mass action [13]. This view was subsequently challenged on the basis that chloroquine concentrations required for lysosomal alkalinization were two orders of magnitude higher than those causing parasite death in malaria [16]. Furthermore, direct pH measurements performed on individual *Plasmodium* parasites cultured under physiological conditions showed a drop in lysosomal pH upon treatment with chloroquine [17]. Thus, the mechanisms of action of chloroquine differ depending on the concentrations applied and the incubation time [18].

Genetics contributed to the study of how chloroquine affects *Plasmodium* revealing that chloroquine-resistant *Plasmodium* strains result from mutations in a lysosomal transporter [19]. Upon mutation, the transporter acquires a novel function to export chloroquine from lysosomes [20, 21]. Chloroquine also binds directly to heme and to the protein complex in the *Plasmodium* food vacuole that is required for hemoglobin degradation and hemozoin formation [22, 23]. In mammalian cells, chloroquine impairs the basal autophagic flux through a decrement of autophagosome-lysosome fusion and not by inhibiting lysosomal degradation [24]. These more recent findings have not fully resolved the mechanism of action for this drug.

The study presented here was initiated at the onset of the Covid19 pandemic and aimed to evaluate the effect of chloroquine on systemic zinc homeostasis in *Drosophila melanogaster*. We previously described that zinc storage in this insect depends on the formation of lysosome-related organelles [25]. We also had information on the endogenous speciation of zinc within the acid granules of the renal-like Malpighian

tubule cells: zinc is complexed predominantly with 3-hydroxy-kynurenine (3HK) and chloride ions [26]. Mutations in the *vermilion* (*v*) gene, which encodes the single tryptophan dioxygenase enzyme in flies, failed to concentrate zinc in the Malpighian tubules of the insect [26]. Considering the known reliance of the immune response on systemic zinc availability [27], we wondered whether chloroquine's mechanism of action was related to zinc homeostasis in flies [28]. Indeed, 300 µM chloroquine is a concentration at the higher end of doses commonly employed and appeared to potentiate the internalization of 50 µM zinc chloride in a human ovarian cancer cell line [29]. Chloroquine was proposed to be a zinc ionophore on this basis [29]. Nevertheless, another report showed that the zinc ionophore clioquinol and chloroquine have contrasting effects on cellular zinc homeostasis, calling for an explanation [30]. More recently, Kavanagh *et al*. showed that hydroxychloroquine does not bind to zinc in physiological conditions, cannot transport zinc through a liposomal membrane in the way known for zinc ionophores, concluding that hydroxychloroquine is not a zinc ionophore [31].

The *Drosophila* model had been used to study the long-term toxicity of chloroquine provoking a myopathy, leading to the discovery that glycogen degradation was partially dependent on the autophagic pathway, which chloroquine inhibits [32]. Therefore, we reasoned that being chloroquine a zinc ionophore, *Drosophila* larvae grown on chloroquine might accumulate more zinc in their granules and v^1 mutant larvae might restore their zinc storage capacity. Furthermore, X-ray absorption near edge structure (XANES) spectroscopy from the Malpighian tubules should reveal a change in zinc speciation corresponding to the newly formed chloroquine-zinc complex. Our experiments also included investigations in Madin-Darby Canine Kidney (MDCK) cells [33], revealing the strong influence of chloroquine in zinc systemic homeostasis and suggesting a surprising additional mechanism of action of chloroquine and its derivatives.

Materials and Methods

Chemicals

Chloroquine diphosphate salt (C6628), zinc chloride (229997) and sodium dodecyl sulphate (SDS, L5750) were purchased from Sigma-Aldrich. Fluozin[TM]-3, AM (F24195), Lysotracker[TM] Deep Red (L7528), penicillin and streptomycin (190846), and trypsin-versene (190510) were purchased from Invitrogen. Metal-free, concentrated (65%) Suprapur nitric acid (1004411000) was from Merck. Dulbecco's modified Eagle's medium (DMEM, 31600-083) and fetal bovine serum with iron (21300-058) were obtained from Life Technologies.

Live material

All experiments were performed with an isogenic *Drosophila melanogaster* w^+ strain, which carries no known mutations [25]. Larvae were grown on media with 12.5 % molasses, 10 % brewer's yeast, 1.6 % agar, 0.3 % gelatin, and 1 % propionic acid in

water. Chloroquine diphosphate and zinc chloride salts were added at final concentrations of 2.5 mg / mL [32] and 1 mM [25], respectively, where indicated.

MDCK cells were grown at 37 °C in an atmosphere of 5% CO_2 and 95% air in DMEM, supplemented with penicillin (10,000 units/ml), streptomycin (10 mg/ml), and 10% fetal bovine serum with iron. After harvesting with trypsin-versene, cells were plated onto multi-well plates (9.6 cm² cell growth area) and incubated for 48 h in supplemented DMEM that was later replaced with a fresh medium containing 50 µM zinc chloride and/or 300 µM chloroquine and incubated for 1 hour at 37°C with continuous agitation.

X-ray absorption experiments

The Malpighian tubules of 22 third instar larvae that were fed during 72 h on a regular diet supplemented with 2.5 mg / mL chloroquine were dissected in a 0.25 M sucrose solution and transferred to a drop of 0.25 M sucrose placed in a Kapton-covered acrylic glass holder. The chloroquine-zinc complex powder was also placed in a similar setup. The sealed holders were frozen in liquid nitrogen and transported to the synchrotron in a pre-chilled Dewar. Other reference samples that appear as key comparators in the figures (Malpighian tubules from control-fed *w⁺* larvae and the complex of zinc with 3-hydroxy-kynurenine and chloride) were handled in the same way and measured during the same beamline session in July 2020 but have been reported before [26]. X-ray absorption spectroscopy (XAS) measurements at the Zn K-edge were performed at the SuperXAS 2.9 T superbending-magnet beamline of the Swiss Light Source (Villigen, Switzerland). The 2.4 GeV storage ring was operated in top-up mode (400 mA) [34]. The source beam was collimated by a Si coated mirror at 2.9 mrad pitch, which also served to reduce higher harmonics, and subsequently monochromatized by a liquid nitrogen cooled channel-cut Si[111] crystal for scanning of the excitation energy. The X-ray beam was focused using a Rh-coated toroidal mirror to a spot size on the sample of 1.5 × 0.3 mm. An energy-resolving five-elements silicon drift detector (RaySpec), shielded by 10 µm Cu foil against scattered incident X-rays was used to determine fluorescence-detected dead time-corrected spectra (one scan of ∼20-min duration per sample spot). Samples were cooled by a stream of liquid nitrogen vapor at ∼100 K. The monochromator energy axis was calibrated using the first inflection point at 9659 eV in the simultaneously measured absorption spectrum of a Zn foil as a standard (accuracy ± 0.1 eV). Averaging (three to six scans per sample), normalization, and extraction of extended X-ray absorption fine structure (EXAFS) oscillations and conversion of the energy scale to the wave-vector (k) scale were performed as previously described [35].

Metal ion measurements

Metal ions were determined using inductively coupled plasma optical emission spectrometry (ICP-OES). Larvae were grown on control and treatment diets as indicated and adult flies of mixed sex were collected between 4 and 7 days after eclosing from pupae. The insects were freeze dried for 8 h to remove water. MDCK cells plated on 9.6 cm² cell growth area (250,000 cells/cm²) were washed 2 times with calcium-free phosphate buffered saline (PBS) after incubation with 50 µM zinc chloride

and/or 300 μM chloroquine and then extracted in 0.2 ml of 1% sodium dodecyl sulphate (SDS).

Twenty milligrams of dry sample (insect bodies) or 0.2 mL of cellular lysate were digested in 1 mL of concentrated (65%) metal-free Suprapur nitric acid at 200 °C for 15 min in closed vessels of the MARS6 microwave digestion system (CEM Corporation). Samples were diluted with Milli-Q water to 5 mL. For the latter set of samples, the blank included 0.2 mL of 1% SDS. Metal ion concentrations were measured against calibration curves and a digestion blank in a PerkinElmer Optima 8300 instrument. Calibration curves were performed for iron and zinc between 0.1 and 5 ppm, for magnesium between 0.5 and 25 ppm, and for potassium between 2 and 100 ppm, so as the measurements to fall within the verified linear range of the respective calibration curves.

Fluorescence imaging

MDCK cells grown on glass coverslips in multi-well plates, were washed 2 times with supplemented DMEM after incubation with 50 μM zinc chloride and/or 300 μM chloroquine and incubated with fresh medium containing 50 nM Lysotracker and 1 μM Fluozin-3 for 30 minutes at 37°C with continuous agitation. After incubation, cells were washed 2 more times with supplemented DMEM and incubated in this medium for additional 30 minutes at 37°C. Cells were then washed 2 times with PBS and mounted in this medium for direct imaging on a TCS SP8 laser confocal microscope (Leica Microsystems). Image processing was on the ImageJ platform.

Freshly dissected Malpighian tubules were incubated for 30 minutes at room temperature in a solution of PBS containing 50 nM Lysotracker, 1 μM Fluozin-3, and 1% fetal bovine serum with iron, washed 2 times with PBS and imaged directly mounted in the same media and imaged in the TCS SP8 laser confocal microscope.

Results

X-ray absorption spectroscopy suggests that chloroquine administration in *Drosophila* reduces zinc stores

Twenty-two pairs of Malpighian tubules were dissected out of control w^+ and mutant v^1 larvae grown on normal diet with or without a 2.5 mg / mL chloroquine treatment and were analyzed by XAS (Figure 1). XAS spectra of the chloroquine-treated w^+ genotype Malpighian tubules suggested significantly lower zinc content (-55.2%) compared to their untreated controls (Figure 1A, B). A similar trend of apparent lower zinc content due to chloroquine treatment was also observed in the v^1 genotype (-34.2%), whose Malpighian tubules show approximately 7.3% of zinc content compared to the w^+ controls under normal conditions (Figure 1B).

The XANES region (Figure 1C left) is very sensitive to small changes in the electronic and geometric structure of zinc and its immediate surrounding. As such, XANES gives great insight into relative changes in zinc speciation as well as new zinc complexes at

physiologically relevant concentrations (>5%). The lower intensity in normalized XANES (white-line) spectra of the v^1 control, as compared to the w^+ control (Figure 1C), is due to the absence of 3HK-zinc-chloride complexes in v^1 mutants [26]. On the other hand, normalized XANES in w^+ and v^1 mutants exhibit a reduced white-line intensity after chloroquine treatment compared to the controls. Similarly, EXAFS, which reflects the first and second sphere coordination surrounding zinc, is different between genotypes but less different between same genotype samples following the chloroquine treatment (Figure 1C right). The induced changes attributed to chloroquine treatment in the spectra could be due to (i) a change in relative zinc speciation due to the resulting reduction in total zinc, which may reflect the varied zinc speciation present in different cellular components [36], or (ii) the formation of a new zinc complex with lower white line intensity. However, comparing spectra of chloroquine-zinc complexes analyzed by the same methodology failed to provide evidence for the appearance of zinc-chloroquine complexes at physiologically relevant concentrations (Figure S1) [37].
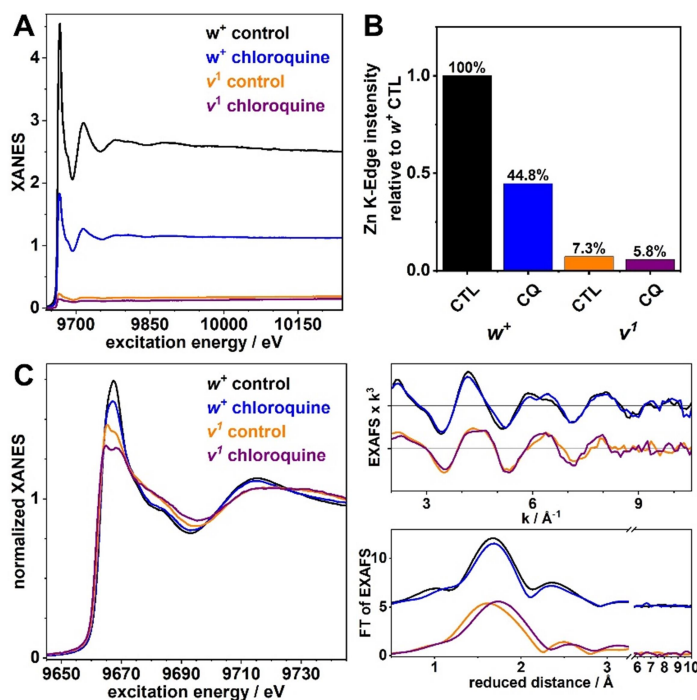

Figure 1. Zinc K-edge X-ray absorption spectra of dissected Malpighian tubules from w^+ and v^1 *Drosophila melanogaster* larvae grown in the absence (control, CTL) or presence (chloroquine, CQ) of 2.5 mg / mL chloroquine. A) XANES without normalization as a measure of relative zinc quantity in the sample. Signal intensity corresponds to fluorescent emission divided by beam intensity prior to sample multiplied by 100000 and background corrected. B) Integral of XANES intensity from A between 9900eV and 10100eV normalized to the w^+ control integral. Relative intensity is indicated for clarity. C) Normalized XANES (left), EXAFS (top right) and Fourier transformed EXAFS spectra (bottom right).

Elemental analysis of *Drosophila* adult flies confirms that chloroquine induced loss of total body zinc

To verify the finding that chloroquine-treated w^+ Malpighian tubules have approximately half zinc content to their controls, we performed elemental analysis on adult flies grown with or without chloroquine. Results of this experiment showed a 37% decrease in total zinc content of flies fed with chloroquine at a concentration of 2.5 mg / mL (Figure 2A). Iron and potassium ions were slightly affected by the same treatment, showing decreases of 7% and 5%, respectively, while magnesium ions were unaffected (Figure 2B-D). These results suggested that the treatment differentially affects zinc storage pools compared to other metal ions. Furthermore, considering that two thirds (67%) of total body zinc content are stored in Malpighian tubules [25, 26], a 55% decrease observed from the synchrotron quantification from the organ-only sample (Figure 1A) expressed as a percent decrease of 67% of the total body zinc, gives a 37% decrease in total body zinc, which fits perfectly with the experimentally observed value (Figure 2A).
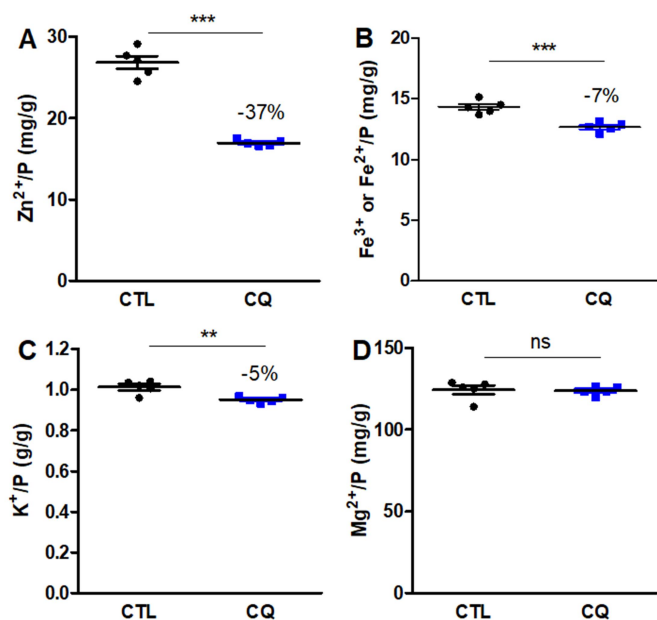

Figure 2. Chloroquine treatment during larval growth results in flies with reduced zinc stores. ICP-OES analysis of whole flies grown on a standard diet (CTL) with or without addition of 2.5 mg / mL chloroquine (CQ). A) The proportion of zinc to phosphorus was diminished by 37% in the chloroquine treatment. B) The proportion of iron to phosphorus was 7% lower in the chloroquine-treated flies. C) The proportion of potassium to phosphorus was 5% lower in the chloroquine-treated flies. D) The proportion of magnesium to phosphorus remained unaffected by the chloroquine treatment. The results from independent batches of lies are shown. Statistical analysis was by unpaired two-tailed t-student test. Three asterisks indicate $p < 0.001$, two asterisks $p < 0.01$.

Our initial experiments were performed with the concentration of chloroquine used previously in the *Drosophila* model [32]. To ask if the response of the Malpighian tubules to dietary chloroquine was dose-responsive, we also fed larvae with increasing concentrations of chloroquine and measured zinc and other ions under these

conditions. The results showed that chloroquine causes a response in a dose-dependent manner (Figure 3A). The experiment served as an independent biological replicate at the concentration of 2.5 mg / mL chloroquine, where the decrease of the zinc to phosphorus ratio was 34%. In the same experiment, the iron to phosphorus ratio showed no changes in response to chloroquine (Figure 3B). There was a trend to lowering total potassium, which reached an 18% drop at 2.5 mg / mL chloroquine (Figure 3C). Magnesium to phosphorus was found 6% lower at the same concentration (Figure 3D). Overall, these results confirm that total body zinc content is highly sensitive to chloroquine concentration in the diet, while potassium ions are also likely affected in whole flies.
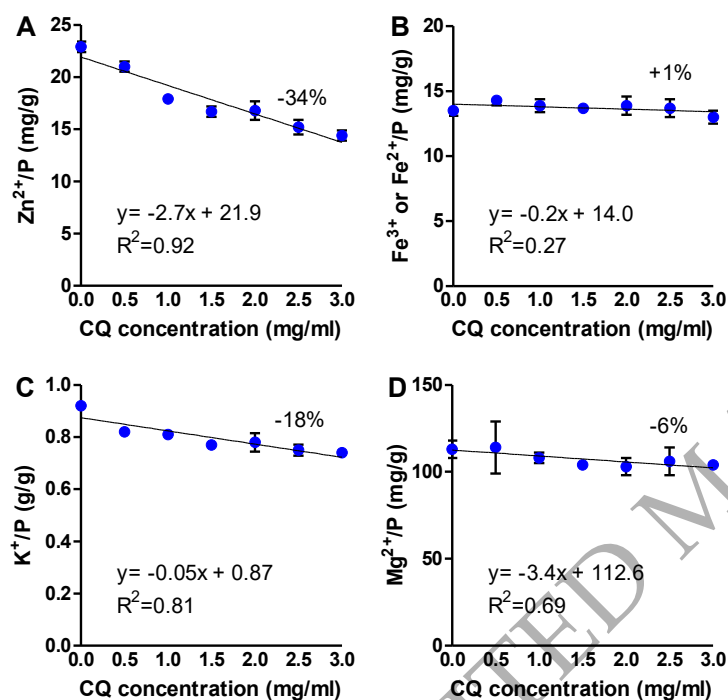

Figure 3. Chloroquine treatment during larval growth results in flies with reduced zinc stores in a dose-dependent manner. ICP-OES analysis of whole flies grown on a standard diet with increasing concentrations of chloroquine. Equations and R^2 values shown are the result of linear regression analysis applied to the data. The percentages indicated show the change with respect to the standard diet at 2.5 mg / mL chloroquine concentration. A) Zinc to phosphorus ratio. B) Iron to phosphorus ratio. C) Potassium to phosphorus ration. D) Magnesium to phosphorus ratio.

Chloroquine treatment of MDCK cells shows an increase in Fluozin-3 fluorescence despite a concomitant loss of intracellular zinc

Our XAS and ICP-OES results call in question whether chloroquine could be a zinc ionophore. This claim resulted from the treatment of a human ovarian cancer cell line with chloroquine and zinc chloride, where zinc concentration was estimated using the Fluozin-3 reporter [29]. Fluorescence from the Fluozin-3-zinc complex is, however, quenched by low pH [38]. Thus, the increase in Fluozin-3 fluorescence intensity following chloroquine treatment could have been the result of a change in pH within

the cellular compartments that contain zinc, a known effect of chloroquine treatment [15, 16]. To address this question, we repeated chloroquine treatments at 300 µM concentration applied to MDCK cells (Figure 4). Our observations confirmed the findings of the previous study, namely that treatment of MDCK cells with 50 µM zinc chloride for one hour had minimal effect on Fluozin-3 fluorescence (Figure 4A, C), in contrast to combined treatment of 300 µM chloroquine and zinc chloride, which resulted in a stark increase of Fluozin-3 fluorescence (Figure 4A, D). We also tested 300 µM chloroquine without addition of exogenous zinc to the cultured media and found that chloroquine alone was sufficient to induce a stark increase of Fluozin-3 fluorescence (Figure 4A, B). A quantification of Fluozin-3 fluorescence showed that its intensity was dependent on chloroquine, but not on exogenous zinc (Figure 5A). Channels are also shown separately to better observe changes of Lysotracker fluorescence upon the respective treatments (Figure S2).
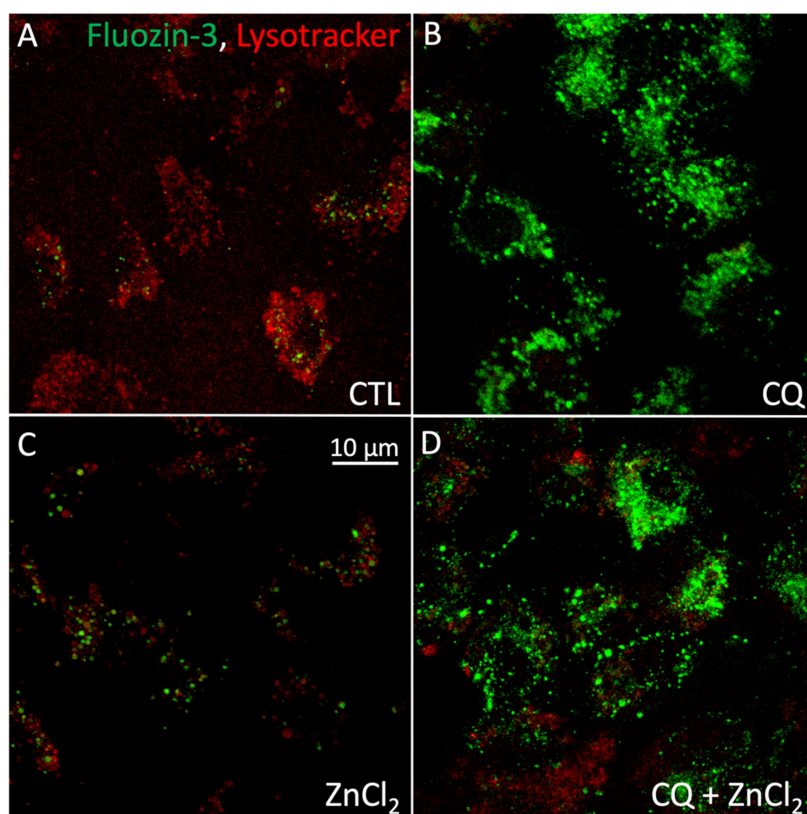

Figure 4. Chloroquine treatment intensifies Fluozin-3 fluorescence observed in subcellular compartments of MDCK cells. A) MDCK cells incubated with Fluozin-3 to observe intracellular zinc and with Lysotracker to monitor acidic intracellular compartments. Note that little colocalization is observed. B) MDCK cells treated for one hour with 300 µM chloroquine. Lysotracker fluorescence appears reduced whereas Fluozin-3 fluorescence is intensified. C) MDCK cells treated for one hour with 50 µM zinc chloride. Fluozin-3 fluorescence is not enhanced. Scale bar is common to all panels. D) MDCK cells treated for one hour with 300 µM chloroquine and 50 µM zinc chloride. Under these conditions Fluozin-3 fluorescence intensifies.

We wondered whether the chloroquine-dependent increase in fluorescence from the reporter could have occurred despite a significant loss of zinc from the zinc storage granule; sufficient zinc remaining in place to still saturate the probe. To address this point, we performed elemental analysis on cell pellets from the same treatments of

MDCK cell cultures. It was immediately evident that cellular zinc concentration was largely decreased by 36% upon exposure of cells with 300 µM chloroquine for one hour (Figure 5B), as observed also in the experiments with whole animals above. Interestingly, treatment with 50 µM zinc chloride for one hour was not sufficient to alter zinc stores in the cells. However, in the presence of such extracellular zinc the treatment with 300 µM chloroquine did not affect intracellular zinc stores (Figure 5B). A comparison of the Fluozin-3 fluorescence quantification (Figure 5A) with the total zinc content of cells (Figure 5B) demonstrates that, on this specific case, the fluorescence of the probe is not primarily determined by cellular zinc concentrations. The results also show that chloroquine should not be considered as a zinc ionophore, as has also been suggested by other investigators [31, 39].
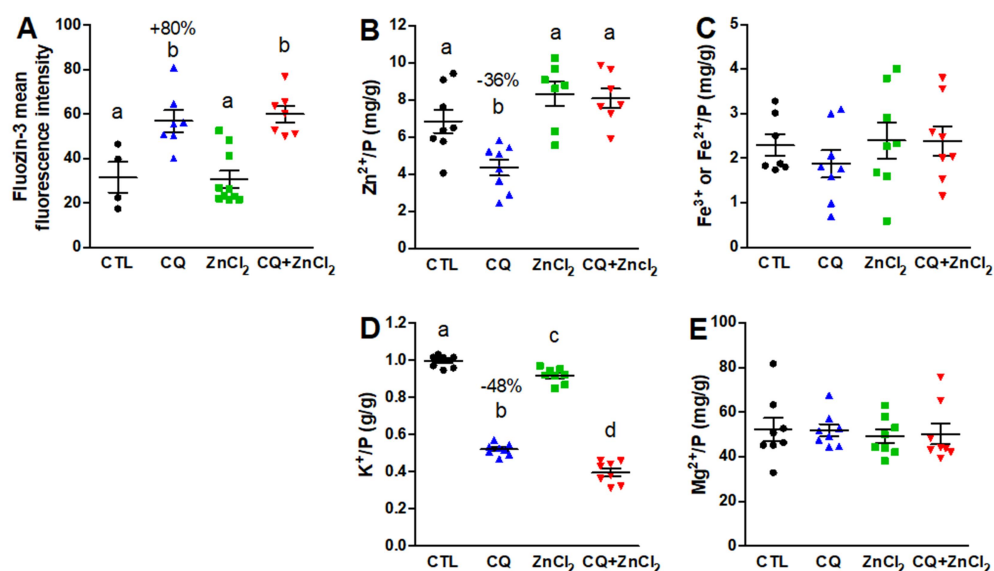

Figure 5. Fluozin-3 fluorescence does not match zinc concentration changes in chloroquine-treated MDCK cells. A) Quantification of Fluozin-3 fluorescence intensity from the experiment shown in Figure 4. Chloroquine treatment induced Fluozin-3 intensity in the presence or absence of additional zinc. Mean fluorescence intensity increased in the chloroquine-only group by 80%. B) Quantification of zinc by ICP-OES in cellular pellets from the same experiment shown in Figure 4. Chloroquine-treated cells showed on average a 36% decrease in their zinc to phosphorus ratio. Zinc chloride treated cells showed no change in intracellular zinc content. Combined treatment of cells with chloroquine and zinc chloride prevented the loss of zinc seen in the chloroquine-only group. C) The iron to phosphorus ratio remained unchanged in all treatments. D) Chloroquine treatment caused a 48% decrease in intracellular potassium ion concentration. Addition of zinc chloride exacerbated this effect. E) As with iron, magnesium to phosphorus treatment remained unaffected in all MDCK cell treatments. Statistical analysis was by one-way ANOVA followed by a Tukey post-hoc test. Different letters indicate statistically significant results ($\alpha < 0.05$).

Elemental analysis further revealed that 300 µM chloroquine had potent effects on intracellular potassium concentration, which was significantly decreased independently of the presence of extracellular zinc chloride (Figure 5D). Iron and magnesium ions, on the other hand, were unaffected by chloroquine or zinc chloride (Figure 5C, E). We were intrigued from the finding that in the presence of extracellular zinc, and despite a clear effect of chloroquine disrupting the lysosomes as illustrated

from Lysotracker fluorescence (Figure 4D, Figure S2), and on potassium ions (Figure 5C), cellular zinc levels remained unaffected (Figure 5B). We therefore decided to test whether something similar occurred in the *Drosophila* model.

Zinc supplementation in parallel with chloroquine corrects intracellular zinc content without reverting chloroquine-induced autophagic defects

We repeated the treatments already applied above (with or without addition 2.5 mg / mL chloroquine) but this time also in the presence of 1 mM zinc chloride added to the diet (Figure 6). In this experiment, exposure of the animals to the chemicals was again throughout larval development and into adulthood, when the flies were collected and analyzed by ICP-OES. As expected, zinc depletion was observed in the chloroquine only group (-46%), but also an increase in zinc storage (+74%) was found in the zinc only group (Figure 6A), the latter finding also expected from a previous report [25]. Interestingly, parallel treatment of 2.5 mg / mL chloroquine and 1 mM zinc chloride resulted in flies that had similar zinc stores to flies grown on normal food (Figure 6A). The ability of zinc supplementation to prevent loss of intracellular zinc from chloroquine, as also supported with the findings from MDCK cells (Figure 5B), suggests that extracellular zinc can compensate or revert the activity of chloroquine to lower intracellular zinc storage.
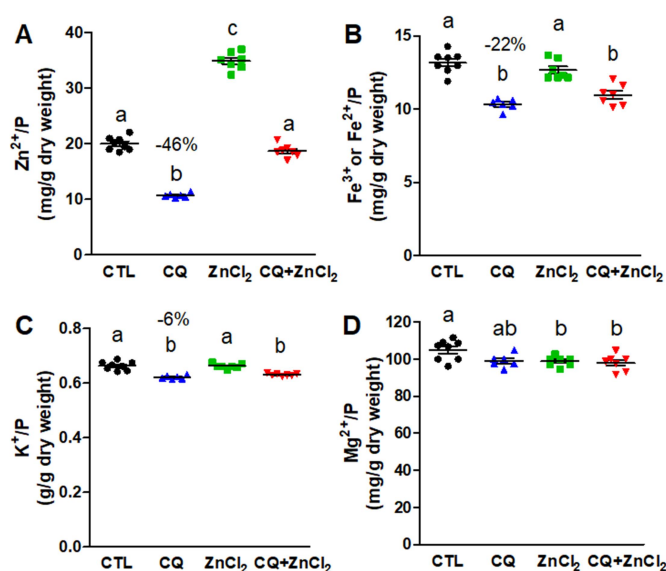

Figure 6. Dietary zinc supplementation of *Drosophila* reverts the loss of intracellular zinc stores caused by chloroquine. A) Chloroquine treatment (2.5 mg / mL) lowered total body zinc (expressed in relation to phosphorus) by 46% but this effect was fully reversed in animals also fed with 1 mM zinc chloride. Larvae exposed to the zinc chloride treatment on its own turned into adults showing a 74% increase in total body zinc content. B) Chloroquine treatment also lowered total body iron by 22% but this effect was not abrogated in the combined treatment group. C) Potassium ions showed a similar pattern to iron, with chloroquine treatment leading to a 6% drop in their whole-body concentration. D) Magnesium ions were only marginally affected by the treatments. Statistical analysis was by one-way ANOVA followed by a Tukey post-hoc test. Different letters indicate statistically significant results ($\alpha < 0.05$).

In these whole-fly elemental analysis experiments, total iron concentration was decreased by -22% (Figure 6B) compared to -7% (Figure 2B) and +1% (Figure 3B) in the previous two independent replicates. Total potassium ion concentration was decreased by -6% (Figure 6C) compared to -5% (Figure 2C) and -18% (Figure 3C). Chloroquine treatment did not lead to statistically significant changes to magnesium content (Figure 6D), as also seen in Figure 2D. We also note that the chloroquine-induced decrease in potassium and iron content was also present in the group of flies that were simultaneously treated with 2.5 mg / mL chloroquine and 1 mM zinc chloride (Figure 6B, C).

A final question was what Fluozin-3 and Lysotracker fluorescence would look like along the Malpighian tubules in the different treatment groups of w^+ larvae. This was particularly interesting given that the combined treatment group restored total body zinc content in adult flies (Figure 6A). Although images of Fluozin-3 fluorescence have been published before from primary cells of Malpighian tubules [25, 26], a description of the fluorescence pattern is lacking in different functional segments of the Malpighian tubules [39, 40]. The initial segment typically lacks Fluozin-3 fluorescence, so we present here images taken from the transitional and main segments (Figure 7). It is evident that different cell types in different regions along the Malpighian tubules show contrasting patterns of Fluozin-3 and Lysotracker fluorescence. The distal part of the transitional segment shows a few cells with large Fluozin-3 fluorescent granules, followed by a more typical pattern of Fluozin-3 fluorescence, interrupted by a few cells with only Lysotracker fluorescence (Figure 7A). The main segment is characterized by two different patterns of fluorescence in primary cells, which either show Fluozin-3 fluorescence (Figure 7E) or Lysotracker fluorescence (Figure 7I). In both these areas of the main segment, stellate cells show cytosolic Fluozin-3 fluorescence. The effect of 2.5 mg / mL chloroquine is most evident with the Lysotracker pattern, showing the accumulation of large autophagic vacuoles (Figure 7B, F, J), consistent with the defects in autophagic flux previously reported by this treatment in *Drosophila* [32] and other systems [10-12, 18, 24]. In some cases, Fluozin-3 and Lysotracker staining colocalize in the enlarged autophagolysosomes, something not frequently observed in Malpighian tubules from larvae grown on standard diet. Growing larvae in 1 mM zinc chloride leads to a Fluozin-3 pattern that is largely similar to that of control larvae, although more intense fluorescence is noted and granules appear to be larger in size (Figure 7C, G, K). Importantly, the double treatment with 2.5 mg / mL chloroquine and 1 mM zinc chloride still showed a large number of enlarged autophagolysosomes throughout the Malpighian tubules, but also showed a much greater extent of Fluozin-3 staining within these abnormal structures (Figure 7D, H, L). From the cytological findings shown in Figure 7, we conclude that the recovery of zinc content in the chloroquine-treated animals supplemented with zinc occurs despite a disrupted autophagy.
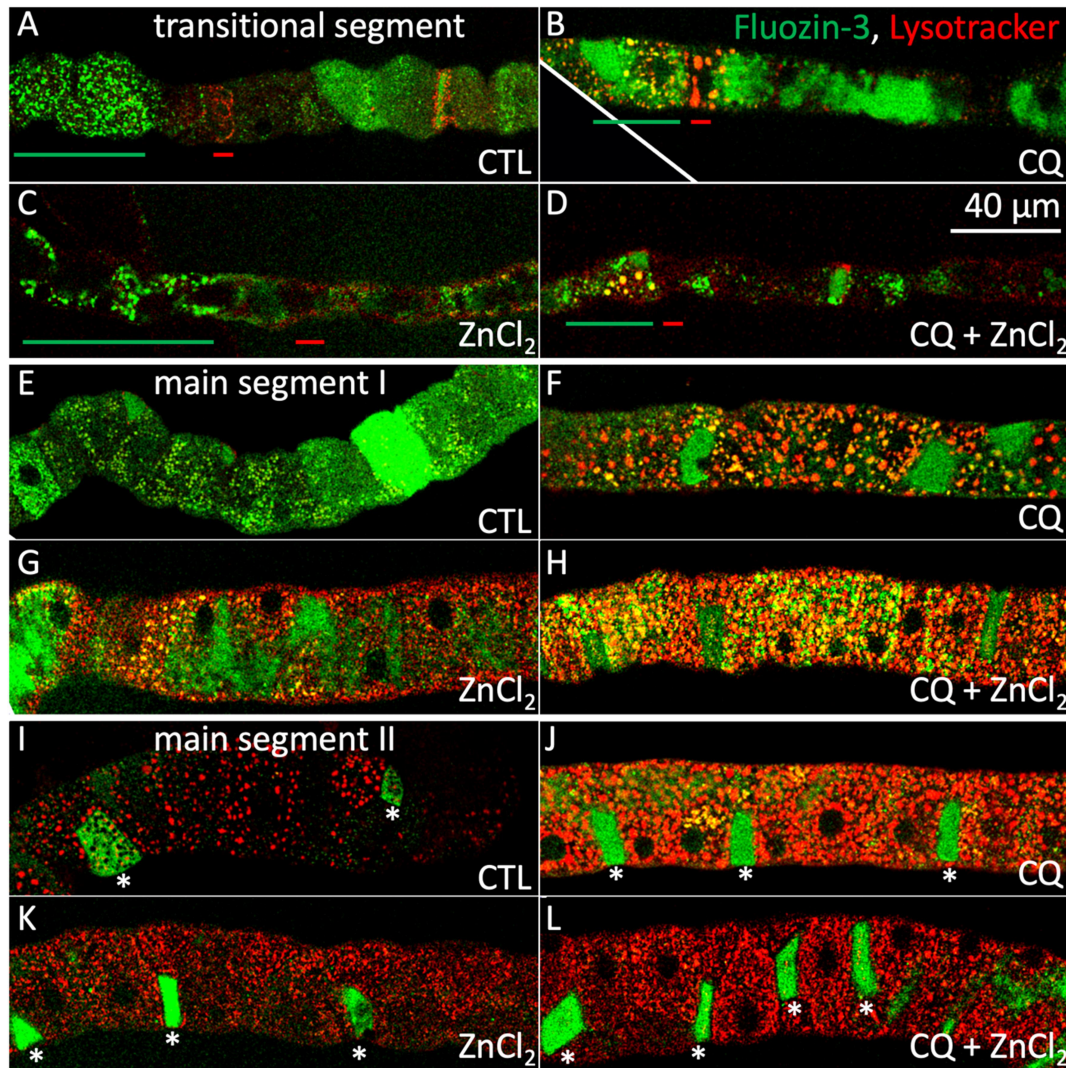
Figure 7. Fluozin-3 and Lysotracker fluorescence in live Malpighian tubules from chloroquine and zinc chloride fed third instar larvae. A) Transitional segment of a w^+ larvae grown under standard diet (CTL). The green bar underlines the region of large zinc storage granules in this region. The red bar underlines the few cells that show exclusively Lysotracker signal. B) Transitional segment of a w^+ larvae grown with 2.5 mg / mL chloroquine (CQ). Note the loss of large zinc storage granules and the abnormal Lysotracker signal indicative of defects in autophagy [32]. C) Transitional segment of a w^+ larvae grown with 1 mM zinc chloride ($ZnCl_2$). The Fluozin-3 and Lysotracker patterns appear similar to CTL, except that zinc storage granules appear larger (green bar). D) Transitional segment of a w^+ larvae that received the combined treatment. Zinc granules are still clearly observable in the distal part of the segment, albeit now colocalizing with Lysotracker fluorescence. The white scale bar representing 40 μM is common for all images taken under the same magnification. E-H) Same treatments as above, this time for the portion of the main segment of the Malpighian tubule where Fluozin-3 fluorescence is normally detected. The autophagic defects of chloroquine are observable by the enlarged size of the Lysotracker positive granules and are not rescued by zinc chloride. I-L) All animals also showed part of the main segment of the Malpighian tubules where no or little Fluozin-3 fluorescence could be seen, except for its presence in stellate cells (indicated with asterisks). In this part of the tubule, the predominant signal is Lysotracker. Once again, the presence of chloroquine in the diet is revealed by the enlarged autophagolysosomes independently of whether the animals were supplemented with zinc chloride or not.

Discussion

Chloroquine is not a zinc ionophore

The original proposal that chloroquine functions to raise intracellular zinc was based on the increased fluorescence observed by the Fluozin-3 reporter in chloroquine-treated cells [29]. Fluozin-3 remains one of the most utilized reporters for intracellular zinc, but as with any fluorescent probe used to quantify metal ions, its utilization requires certain precautionary considerations [38]. It is prudent to consider the probe´s affinity and specificity for the metal ion and whether fluorescence is dependent on the probe's concentration and on other chemical interferences, such as changes in pH [38].

Previous research showed that chloroquine treatment arrested autophagy in adult retinal pigment epithelial cells, but the zinc ionophore clioquinol attenuated autophagolysosomal formations in a zinc-dependent manner [30]. Contrasting findings between clioquinol and chloroquine treatments were also reported more recently in lung epithelial cells [31]. Application of extracellular zinc with clioquinol was lethal to these cells, whereas hydroxychloroquine treatment had no observable adverse effect [31]. Zinc binds to chloroquine with low affinity and its mode of coordination depends on chemical environment [37]. Experiments with purified liposomes showed no evidence for ionophore activity, in the context of crossing a phospholipid bilayer, leading others to conclude that hydroxychloroquine is not a zinc ionophore [31]. Moreover, while African green monkey kidney cells treated with chloroquine showed increased Fluozin-3 fluorescence, they showed no change in fluorescence with the cytosolic Zinquin fluorophore, suggesting that chloroquine was not acting as a zinc ionophore [39]. The actual quantifications of the zinc metal ion in chloroquine-treated cells presented here settle this issue conclusively, as chloroquine treatment was found to cause, in fact, significant loss of intracellularly stored zinc, an inconsistent result with the proposal that chloroquine acts a zinc ionophore. Conversely, our findings are consistent with all the experiments reported above, considering the fluorescent properties of the Fluozin-3-zinc complex [38]. One aspect that requires further investigation is the detailed mechanism of release for zinc from cells [41, 42].

Chloroquine treatment disrupts intracellular storage of zinc and other ions

Drosophila melanogaster adult flies grown as larvae on media with 2.5 mg / mL chloroquine were invariably found to contain less total body zinc. The magnitude of this loss varied between 34-46% between independent experiments. Interestingly, a one-hour treatment of MDCK cells with 300 μM chloroquine also resulted in a similar 36% loss of total zinc. In MDCK cells treated with chloroquine, potassium ions were also greatly affected to an even greater level of -48%. A recent medical case of a child that accidentally ingested 10 g of hydroxychloroquine resulted in hypokalemia [43], a well-documented effect for high dosages of chloroquine [44]. The proposed mechanism for chloroquine's action in causing hypokalemia is its direct binding and inhibition of potassium channels [45-47], or by Na^+K^+-ATPase inhibition [48, 49]. With respect to the latter mechanism, chloroquine has been shown to affect binding of the

Na$^+$K$^+$-ATPase inhibitor ouabain to the pump and affect the recovery of cells from ouabain treatments [50, 51]. In the present study, we have not focused on the effects of chloroquine on potassium ions, but it is worth noting that, along with zinc, potassium was the only other ion that was decreased in all three experiments in our *in vivo* model, consistent with what was already known from medical experience.

Hydroxychloroquine treatment may lead to depleted intracellular zinc stores

The main outcome of this study is that chloroquine treatment leads to the depletion of zinc from intracellular storage sites. This conclusion has implications for the mechanism of action of the drug in disease and may help explain early findings during the use hydroxychloroquine as an antiviral agent in Covid19, where zinc supplementation seemed to offer a certain level of protection from lethality [52, 53]. Of particular interest, however, is to address whether co-supplementation of zinc and potassium would improve the effectiveness of hydroxychloroquine in its common use against autoimmune disease [7, 8]. In this respect, it was recently proposed that kynurenine may act as a peripheral signal to remove zinc from circulation into intracellular deposits [26]. This proposal comes primarily from work in *Drosophila* and still needs to be tested in the context of human physiology, but it is notable that patients with lupus erythematosus show increased kynurenine concentration in their blood [54-57] and lower zinc serum concentration [58-60]. Although the etiology of autoimmune disease is complex [61-63], our findings here suggest that the therapeutic mechanism of action of hydroxychloroquine might be through direct counteracting of the newly proposed kynurenine activity with respect to systemic zinc homeostasis [26].

References

1. R. F. Loeb, W. M. Clark, G. R. Coatney, L. T. Coggeshall, F. R. Dieuaide, A. R. Dochez, E. G. Hakansson, E. K. Marshal Jr., C. S. Marvel, O. R. McCoy, J. J. Sapero, W. H. Sebrell, J. A. Shannon, G. A. Carden Jr., Activity of a new antimalarial agent, chloroquine (SN 7618), *J. Am. Med. Assoc.*, 1946, **130**, 1069-1070.
2. G. G. Haydu, Rheumatoid arthritis therapy; a rationale and the use of chloroquine diphosphate, *J. Am. Med. Assoc.*, 1953, **225**, 71-75.

3. J. C. Shee, Lupus erythematosus treated with chloroquine, *Lancet*, 1953, **265**, 201-202.

4. J. L. Smith, Chloroquine macular degeneration, *Arch. Ophtalmol.*, 1962, **54**, 381-385.

5. B. Smith, F. O'Grady, Experimental chloroquine myopathy, *J. Neurol. Neurosurg. Psychiatry*, 1966, **29**, 255-258.

6. RECOVERY Collaborative Group, P. Horby, M. Mafham, L. Linsell, J. L. Bell, N. Staplin, J. R. Emberson, M. Wiselka, A. Ustianowski, E. Elmahi, B. Prudon, T. Whitehouse, T. Felton, J. Williams, J. Faccenda, J. Underwood, J. K. Baillie, L. C. Chappell, S. N. Faust, T. Jaki, K. Jeffery, W. S. Lim, A. Montgomery, K. Rowan, J. Tarning, J. A. Watson, N. J. White, E. Juszczak, R. Haynes, M. J. Landray, Effect of Hydroxychloroquine in Hospitalized Patients with Covid-19, *N. Engl. J. Med.*, 2020, **383**, 2030-2040.

7. A. Fanouriakis, M. Kostopoulou, A. Alunno, M. Aringer, I. Bajema, J. N. Boletis, R. Cervera, A. Doria, C. Gordon, M. Govoni, F. Houssiau, D. Jayne, M. Kouloumas, A. Kuhn, J. L. Larsen, K. Lerstrøm, G. Moroni, M. Mosca, M. Schneider, J. S. Smolen, E. Svenungsson, V. Tesar, A. Tincani, A. Troldborg, R. van Vollenhoven, J. Wenzel, G. Bertsias, D. T. Boumpas, 2019 update of the EULAR recommendations for the management of systemic lupus erythematosus, *Ann. Rheum. Dis.*, 2019, **78**, 736-745.

8. E. L. Nirk, F. Reggiori, M. Mauthe, Hydroxychloroquine in rheumatic autoimmune disorders and beyond, *EMBO Mol. Med.*, 2020, **12**, e12476.

9. L. Hopkinson, F. L. Jackson, Effects of chloroquine on growth and metabolism, *Nature*, 1964, **202**, 27-29.

10. R. Abraham, R. Hendy, P. Grasso, Formation of myeloid bodies in rat liver lysosomes after chloroquine administration, *Exp. Mol. Pathol.*, 1968, **9**, 212-229.

11. S. O. Lie, B. Schofield, Inactivation of lysosomal function in normal cultured human fibroblasts by chloroquine, *Biochem. Pharmacol.*, 1973, **22**, 3109-3112.

12. D. C. Warhurst, D. J. Hockley, Mode of action of chloroquine on Plasmodium berghei and P. cynomologi, *Nature*, 1967, **214**, 935-936.

13. C. A. Homewood, D. C. Warhurst, W. Peters, V. C. Baggaley, Lysosomes, pH and the anti-malarial action of chloroquine, *Nature*, 1972, **235**, 50-52.

14. C. De Duve, T. De Barsy, B. Poole, A. Trouet, P. Tulkens, F. Van Hoof, Lysosomotropic agents, *Biochem. Pharmacol.*, 1974, **23**, 2495-2531.

15. D. J. Krogstad, P. H. Schlesinger, I. Y. Gluzman, Antimalarials increase vesicle pH in Plasmodium falciparum, *J. Cell Biol.*, 1985, **101**, 2302-2309.

16. H. Ginsburg, E. Nissani, M. Krugliak, Alkalinization of the food vacuole of malaria parasites by quinoline drugs and alkylamines is not correlated with their antimalarial activity, *Biochem. Pharmacol.*, 1989, **38**, 2645-2654.

17. L. M. B. Ursos, S. M. Dzekunov, P. D. Roepe, The effects of chloroquine and verapamil on digestive vacuolar pH of P. falciparum either sensitive or resistant to chloroquine. *Mol. Biochem. Parasitol.*, 2000, **110**, 125-134.

18. S. Lu, T. Sung, N. Lin, R. T. Abraham, B. A. Jessen, Lysosomal adaptation: How cells respond to lysosomotropic compounds, *PLoS one*, 2017, **12**, e0173771.

19. D. A. Fidock, T. Nomura, A. K. Talley, R. A. Cooper, S. M. Dzekunov, M. T. Ferdig, L. M. Ursos, A. B. Sidhu, B. Naudé, K. W. Deitsch, X. Z. Su, J.C. Wootton, P. D.

Roepe, T. E. Wellems, Mutations in the P. falciparum digestive vacuole transmembrane protein PfCRT and evidence for their role in chloroquine resistance, *Mol. Cell*, 2000, **6**, 861-871.

20. R. E. Martin, R. V. Marchetti, A. I. Cowan, S. M. Howitt, S. Bröer, K. Kirk, Chloroquine transport via the malaria parasite's chloroquine resistance transporter, *Science*, 2009, **325**, 1680-1682.

21. J. Kim, Y. Z. Tan, K. J. Wicht, S. K. Erramilli, S. K. Dhingra, J. Okombo, J. Vendome, L. M. Hagenah, S. I. Giacometti, A. L. Warren, K. Nosol, P. D. Roepe, C. S. Potter, B. Carragher, A. A. Kossiakoff, M. Quick, D. A. Fidock, F. Mancia, Structure and drug resistance of the Plasmodium falciparum transporter PfCRT, *Nature*, 2019, **576**, 315-320.

22. Pandey AV, Bisht H, Babbarwal VK, Srivastava J, Pandey KC, Chauhan VS, Mechanism of malarial haem detoxification inhibition by chloroquine, *Biochem J*, 2001, **355**, 333-338.

23. Chugh M, Sundararaman V, Kumar S, Reddy VS, Siddiqui WA, Stuart KD, Malhotra P, Protein complex directs hemoglobin-to-hemozoin formation in Plasmodium falciparum, *Proc. Natl. Acad. Sci. U. S. A.*, 2013, **110**, 5392-5397.

24. M. Mauthe, I. Orhon, C. Rocchi, X. Zhou, M. Luhr, K. J. Hijlkema, R. P. Coppesa, N. Engedal, M. Mari, F. Reggiori, Chloroquine inhibits autophagic flux by decreasing autophagosome-lysosome fusion, *Autophagy*, 2018, **14**, 1435-1455.

25. C. Tejeda-Guzman, A. Rosas-Arellano, T. Kroll, S. M. Webb, M. Barajas-Aceves, B. Osorio and F. Missirlis, Biogenesis of zinc storage granules in Drosophila melanogaster, *J. Exp. Biol.*, 2018, **221**, jeb168419.

26. E. Garay, N. Schuth, A. Barbanente, C. Tejeda-Guzmán, D. Vitone, B. Osorio, A. H. Clark, M. Nachtegaal, M. Haumann, H. Dau, A. Vela, F. Arnesano, L. Quintanar, F. Missirlis, Tryptophan regulates Drosophila zinc stores, *Proc. Natl. Acad. Sci. U. S. A.*, 2022, **119**, e2117807119.

27. I. Wessels, H. J. Fischer, L. Rink, Dietary and Physiological Effects of Zinc on the Immune System, *Annu. Rev. Nutr.*, 2021, **41**, 133-175.

28. G. Xiao, Molecular physiology of zinc in Drosophila melanogaster, *Curr. Opin. Insect Sci.*, 2022, **51**, 100899.

29. J. Xue, A. Moyer, B. Peng, J. Wu, B. N. Hannafon, W. Q. Ding, Chloroquine is a zinc ionophore, *PLOS one*, 2014, **9**, e109180.

30. B. R. Seo, S. J. Lee, K. S. Cho, Y. H. Yoon, J. Y. Koh, The zinc ionophore clioquinol reverses autophagy arrest in chloroquine-treated ARPE-19 cells and in APP/mutant presenilin-1-transfected Chinese hamster ovary cells, *Neurobiol. Aging*, 2015, **36**, 3228-3238.

31. O. N. Kavanagh, S. Bhattacharya, L. Marchetti, R. Elmes, F. O'Sullivan, J. P. Farragher, S. Robinson, D. Thompson, G. M. Walker, Hydroxychloroquine does not function as a direct zinc ionophore, *Pharmaceutics*, 2022, **14**, 899.

32. J. Zirin, J. Nieuwenhuis, N. Perrimon, Role of autophagy in glycogen breakdown and its relevance to chloroquine myopathy, *PLOS Biol.*, 2013, **11**, e1001708.

33. V. García-Hernández, C. Flores-Maldonado, R. Rincon-Heredia, O. Verdejo-Torres, J. Bonilla-Delgado, I. Meneses-Morales, P. Gariglio, R. G. Contreras, EGF regulates claudin-2 and -4 expression through Src and STAT3 in MDCK cells, *J. Cell. Physiol.*, 2015, **230**, 105-115.

34. O. Müller, M. Nachtegaal, J. Just, D. Lützenkirchen-Hecht, R. Frahm, Quick-EXAFS setup at the SuperXAS beamline for in situ X-ray absorption spectroscopy with 10 ms time resolution, *J. Synchrotron Radiat.*, 2016, **23**, 260-266.

35. N. Schuth, S. Mebs, D. Huwald, P. Wrzolek, M. Schwalbe, A. Hemschemeier, M. Haumann, Effective intermediate-spin iron in O2-transporting heme proteins, *Proc. Natl. Acad. Sci. U.S.A.*, 2017, **114**, 8556–8561.

36. G. Wellenreuther, M. Cianci, R. Tucoulou, W. Meyer-Klaucke, H. Haase, The ligand environment of zinc stored in vesicles, *Biochem. Biophys. Res. Commun.*, 2009, **380**, 198-203.

37. M. Paulikat, D. Vitone, F. K. Schackert, Nils Schuth, A. Barbanente, G. M. Piccini, E. Ippoliti, G. Rossetti, A. H. Clark, M. Nachtegaal, M. Haumann, H. Dau, P. Carloni, S. Geremia, R. De Zorzi, L. Quintanar, F. Arnesano, Molecular dynamics and structural studies of zinc chloroquine complexes, *ChemRxiv*, 2022, 10.26434/chemrxiv-2022-d9pjp-v2.

38. I. Marszałek, A. Krężel, W. Goch, I. Zhukov, I. Paczkowska, W. Bal, Revised stability constant, spectroscopic properties and binding mode of Zn(II) to FluoZin-3, the most common zinc probe in life sciences, *J. Inorg. Biochem.*, 2016, **161**, 107-114.

39. M. Vogel-González, M. Talló-Parra, V. Herrera-Fernández, G. Pérez-Vilaró, M. Chillón, X. Nogués, S. Gómez-Zorrilla, I. López-Montesinos, I. Arnau-Barrés, M. L. Sorli-Redó, J. P. Horcajada, N. García-Giralt, J. Pascual, J. Díez, R. Vicente, R. Güerri-Fernández, Low Zinc Levels at Admission Associates with Poor Clinical Outcomes in SARS-CoV-2 Infection, *Nutrients*, 2021, **13**, 562.

40. J. Xu, Y. Liu, H. Li, A. J. Tarashansky, C. H. Kalicki, R. J. Hung, Y. Hu, A. Comjean, S. S. Kolluru, B. Wang, S. R. Quake, L. Luo, A. P. McMahon, J. A. T. Dow, N. Perrimon, Transcriptional and functional motifs defining renal function revealed by single-nucleus RNA sequencing, *Proc. Natl. Acad. Sci. U. S. A.*, 2022, **119**, e2203179119.

41. S. Yin, Q. Qin, B. Zhou, Functional studies of Drosophila zinc transporters reveal the mechanism for zinc excretion in Malpighian tubules, *BMC Biol.*, 2017, **15**, 12.

42. N. McCormick, V. Velasquez, L. Finney, S. Vogt, S. L. Kelleher, X-Ray fluorescence microscopy reveals accumulation and secretion of discrete intracellular zinc pools in the lactating mouse mammary gland, *PLoS one*, 2010, **5**, e11078.

43. P. Srihari, A. B. Minns, H. T. Gao, A. A. Kreshak, Massive nonfatal hydroxychloroquine ingestion in a pediatric patient, *J. Emerg. Med.*, 2022, **62**, 332-336.

44. J. L. Clemessy, C. Favier, S. W. Borron, P. E. Hantson, E. Vicaut, F. J. Baud, Hypokalaemia related to acute chloroquine ingestion, *Lancet*, 1995, **346**, 877-880.

45. A. A. Rodríguez-Menchaca, R. A. Navarro-Polanco, T. Ferrer-Villada, J. Rupp, F. B. Sachse, M. Tristani-Firouzi, J. A. Sánchez-Chapula, The molecular basis of chloroquine block of the inward rectifier Kir2.1 channel, *Proc. Natl. Acad. Sci. U. S. A.*, 2008, **105**, 1364-1368.

46. Y. Takemoto, D. P. Slough, G. Meinke, C. Katnik, Z. A. Graziano, B. Chidipi, M. Reiser, M. M. Alhadidy, R. Ramirez, O. Salvador-Montañés, S. Ennis, G. Guerrero-Serna, M. Haburcak, C. Diehl, J. Cuevas, J. Jalife, A. Bohm, Y. S. Lin, S. F. Noujaim, Structural basis for the antiarrhythmic blockade of a potassium channel with a small molecule, *FASEB J.*, 2018, **32**, 1778-1793.

47. M. Szendrey, J. Guo, W. Li, T. Yang, S. Zhang, COVID-19 Drugs chloroquine and hydroxychloroquine, but not azithromycin and remdesivir, block hERG potassium channels, *J. Pharmacol. Exp. Ther.*, 2021, **377**, 265-272.

48. S. Chandra, G. Adhikary, R. Sikdar, P. C. Sen, The in vivo inhibition of transport enzyme activities by chloroquine in different organs of rat is reversible, *Mol. Cell. Biochem.,* 1992, **118**, 15–21.

49. B. Huang, N. Meng, B. Zhao, J. Zhao, Y. Zhang, S. Zhang, J. Miao, Protective effects of a synthesized butyrolactone derivative against chloroquine-induced autophagic vesicle accumulation and the disturbance of mitochondrial membrane potential and Na+, K+-ATPase activity in vascular endothelial cells, *Chem. Res. Toxicol.,* 2009*,* **22**, 471–475.

50. R. G. Contreras, G. Avila, C. Gutierrez, J. J. Bolívar, L. González-Mariscal, A. Darzon, G. Beaty, E. Rodriguez-Boulan, M. Cereijido, Repolarization of Na + -K + pumps during establishment of epithelial monolayers, *Am. Physiol. Soc.,* 1989 **257**, C896-905.

51. R. G. Contreras, A. Lázaro, A. Mújica, L. González-Mariscal, J. Valdés, M. R. García-Villegas, M. Cereijido, Ouabain resistance of the epithelial cell line (Ma104) is not due to lack of affinity of its pumps for the drug, *J. Membr. Biol.,* 1995 **145**, 295–303.

52. P. M. Carlucci, T. Ahuja, C. Petrilli, H. Rajagopalan, S. Jones, J. Rahimian, Zinc sulfate in combination with a zinc ionophore may improve outcomes in hospitalized COVID-19 patients, *J. Med. Microbiol.*, 2020, **69**, 1228–1234.

53. R. Derwand, M. Scholz, V. Zelenko, N. York, COVID-19 outpatients—Early risk-stratified treatment with zinc plus low dose hydroxychloroquine and azithromycin: A retrospective case series study, *Int. J. Antimicrob. Agents*, 2020, **56**, 106214.

54. B. Widner, N. Sepp, E. Kowald, S. Kind, M. Schmuth, D. Fuchs, Degradation of tryptophan in patients with systemic lupus erythematosus, *Adv. Exp. Med. Biol.*, 1999, **467**, 571-577.

55. M. Pertovaara, T. Hasan, A. Raitala, S. S. Oja, U. Yli-Kerttula, M. Korpela, M. Hurme, Indoleamine 2,3-dioxygenase activity is increased in patients with systemic lupus erythematosus and predicts disease activation in the sunny season, *Clin. Exp. Immunol.*, 2007, **150**, 274-278.

56. A. Perl, R. Hanczko, Z. W. Lai, Z. Oaks, R. Kelly, R. Borsuk, J. M. Asara, P. E. Phillips, Comprehensive metabolome analyses reveal N-acetylcysteine-responsive accumulation of kynurenine in systemic lupus erythematosus: implications for activation of the mechanistic target of rapamycin, *Metabolomics*, 2015, **11**, 1157-1174.

57. K. Åkesson, S. Pettersson, S. Ståhl, I. Surowiec, M. Hedenström, S. Eketjäll, J. Trygg, P. J. Jakobsson, I. Gunnarsson, E. Svenungsson, H. Idborg, Kynurenine pathway is altered in patients with SLE and associated with severe fatigue, *Lupus Sci. Med.*, 2018, **5**, e000254.

58. M. Sahebari, M. Abrishami-Moghaddam, A. Moezzi, M. Ghayour-Mobarhan, Z. Mirfeizi, H. Esmaily, G. Ferns, Association between serum trace element concentrations and the disease activity of systemic lupus erythematosus, *Lupus*, 2014, **23**, 793-801.

59. C. N. Tóth, E. Baranyai, I. Csípő, T. Tarr, M. Zeher, J. Posta, I. Fábián, Elemental Analysis of Whole and Protein Separated Blood Serum of Patients with Systemic Lupus Erythematosus and Sjögren's Syndrome, *Biol. Trace Elem. Res.*, 2017, **179**, 14-22.

60. H. Wang, X. B. Li, R. G. Huang, N. W. Cao, H. Wu, K. D. Li, Y. Y. Wang, B. Z. Li, Essential Trace Element Status in Systemic Lupus Erythematosus: a Meta-analysis Based on Case-Control Studies, *Biol. Trace Elem. Res.*, 2022, doi: 10.1007/s12011-022-03335-y.

61. F. Rosetti, I. K. Madera-Salcedo, N. Rodríguez-Rodríguez, J. C. Crispín, Regulation of activated T cell survival in rheumatic autoimmune diseases, *Nat. Rev. Rheumatol.*, 2022, **18**, 232-244.

62. M. Terrell, L. Morel, The Intersection of Cellular and Systemic Metabolism: Metabolic Syndrome in Systemic Lupus Erythematosus, *Endocrinology*, 2022, **163**, bqac067.

63. P. Karagianni, A. G. Tzioufas, Epigenetic perspectives on systemic autoimmune disease, *J. Autoimmun.*, 2019, **104**, 102315.